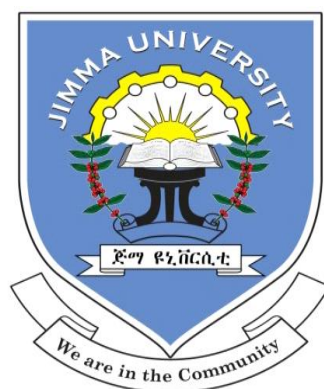


**JIMMA UNIVERSITY**

**SCHOOL OF GRADUATE STUDIES**

**COLLEGE OF NATURAL SCIENCE**

**DEPARTMENT OF CHEMISTRY**



**THESIS**

**ON**

**DEFECT INDUCED BAND GAP NARROWING OF ZINC OXIDE  
NANOPARTICLES USING  $\text{Li}^+$ ,  $\text{Na}^+$  AND  $\text{K}^+$  METAL IONS AS A DOPANT**

**JUNE, 2015  
JIMMA, ETHIOPIA**

**DEFECT INDUCED BAND GAP NARROWING OF ZINC OXIDE  
NANOPARTICLES USING Li<sup>+</sup>, Na<sup>+</sup> AND K<sup>+</sup> METAL IONS AS A DOPANT**

**A RESEARCH THESIS SUBMITTED TO SCHOOL OF GRADUATE  
STUDIES JIMMA UNIVERSITY IN PARTIAL FULFILLMENT OF THE  
REQUIREMENTS FOR THE DEGREE OF MASTER OF SCIENCE IN  
CHEMISTRY**

**By**

**TIZITA GIRMA**

**ADVISOR: KHALID SIRAJ (PhD)**

**CO-ADVISOR: ALEMAYEHU YIFRU (MSc)**

**A RESEARCH THESIS SUBMITTED TO SCHOOL OF GRADUATE  
STUDIES JIMMA UNIVERSITY IN PARTIAL FULFILLMENT OF THE  
REQUIREMENTS FOR THE DEGREE OF MASTER OF SCIENCE IN  
CHEMISTRY**

<b>Advisor</b>	Signature	Date
Khalid Siraj (PhD) Department of Chemistry College of Natural Sciences, Jimma University	.....	.....
<b>Co- Advisor</b> Alemayehu Yifru (Msc) Department of Chemistry College of Natural Sciences, Jimma University	.....	.....
<b>Examiner</b> Gezahegn Faye () Department of Chemistry College of Natural Sciences, Jimma University	.....	.....

## Table of Contents

Table of Contents .....	iii
List of Abbreviations and Symbols.....	iv
List of Figures .....	v
List of Tables .....	vi
Acknowledgement .....	vii
Abstract .....	viii
1. INTRODUCTION .....	9
2. REVIEW LITERATURE .....	12
2.1. Doping.....	12
2.1.1. Optical properties .....	14
2.1.2. Effect of doping on band gap energy .....	15
2.2. Statement of the problems.....	12
2.3. Objectives of the study.....	17
2.3.1. General objective.....	17
2.3.2. Specific objectives.....	17
2.4. Significance of the study .....	18
3. MATERIALS AND METHODS.....	19
3.1. Chemicals .....	19
3.1.1 Instrument and materials .....	19
3.2. Procedures .....	19
3.2.1. Preparation of ZnO nanoparticles .....	19
3.2.2. Preparation of Sodium, lithium and potassium ions doped ZnO nanoparticles .....	19
4. RESULTS AND DISCUSSION .....	20
4.1. Absorption spectrum .....	20
4.1.1. Characterization of ZnO nanoparticles .....	20
4.2. Optical properties of different concentration of Li <sup>+</sup> , Na <sup>+</sup> and K <sup>+</sup> doped ZnO .....	23
4.2.1. Characterization of Li <sup>+</sup> , Na <sup>+</sup> and K <sup>+</sup> doped ZnO nanoparticles .....	23
4.3. Effect of doping on band gap energy of ZnO nanoparticles .....	25
4.4. Comparison of the obtained results with reported values.....	28
5. CONCLUSSION.....	29
References.....	30

## List of Abbreviations and Symbols

AEM	Alkaline Earth Metal
AM	Alkali metal
DSSCs	Dye-sensitized solar cells
ITO	Indium Thin Oxide
KZO	Potassium zinc oxide
LZO	Lithium zinc oxide
NZO	Sodium zinc oxide
TFTs	Thin film transistors

## List of Figures

Fig1: The differences between Materials.....	11
Fig 2: The difference between N and P type dopants .....	13
Fig 3: UV-vis absorption spectrum of ZnO nanoparticles.....	20
Fig 4: Plots of $\alpha h\nu^2$ versus photon energy ( $h\nu$ ) of ZnO nanoparticles.....	21
Fig 5: The UV–Visible absorption spectra of a) $\text{Li}^+$ , b) $\text{Na}^+$ and c) $\text{K}^+$ doped and undoped ZnO nanoparticles .....	24
Fig 6:Plots of $(\alpha h\nu)^2$ vs $h\nu$ for undoped ZnO nanoparticles and different concentrations of a) $\text{Li}^+$ , b) $\text{Na}^+$ and c) $\text{K}^+$ doped ZnO nanoparticles .....	25

## List of Tables

Table 1: Maximum absorption peaks of different concentration doped ZnO nanoparticles .....	24
Table 2: The band gap energy of undoped and different conc. of Li <sup>+</sup> , Na <sup>+</sup> and K <sup>+</sup> doped ZnO nanoparticles.....	27
Table 3: Comparative study of Li <sup>+</sup> and K <sup>+</sup> doped ZnO thin films from literature and doped ZnO nanoparticles for this work.....	29

## **Acknowledgement**

Above all, I would like to offer enormous thanks to almighty God for his help throughout my work according to his good will. Next, I would like to forward my deepest appreciation to my advisor Khalid Siraj (PhD) for his patience advice and my co-advisor Alemayehu Yifru (MSc). I also owe great gratitude to my family for their finance and moral support and all my friends for their moral support. I acknowledge; Dr. Abera Gure and Dr. Yared Merdassa for their support throughout my work. Last but not least I would like to express my appreciation to Department of Chemistry and all lab technicians, Jimma University.



## Abstract

ZnO nanoparticles have been synthesized by precipitation method from zinc acetate dihydrate and sodium hydroxide. The obtained precipitated compound was calcined at 400<sup>0</sup> C for 2 hr and then, the obtained product was dissolved in deionized water. The prepared solution was characterized by UV-visible spectrophotometer and it was show absorption maxima at 380 nm and particle size of 3.6 nm that was almost equal to 4 nm, not exhibiting band gap enlargement. The band gap energy was lower for synthesized ZnO nanoparticles (3.263eV) than their bulk counterparts (3.37 eV), indicating high conductivity than the bulk ZnO powder. Zn<sub>1-x</sub>Li<sub>x</sub>O, Zn<sub>1-x</sub>Na<sub>x</sub>O and Zn<sub>1-x</sub>K<sub>x</sub>O (where x= 0.005, 0.01, 0.015 and 0.02 M for all dopants) doped ZnO nanoparticles was prepared and calcined at 400<sup>0</sup>C for 2 hr and their solution was then characterized by UV-vis spectrophotometer. All concentration of Li<sup>+</sup> doped ZnO nanoparticles was more narrowing the band gap of the undoped ZnO nanoparticles than Na<sup>+</sup> and K<sup>+</sup> doped ZnO nanoparticles. Both the size and concentration of dopants were affecting the band gap energy of ZnO nanoparticles. As the concentration and ionic radii of the dopants increases the optical band gap energy was also increasing. So the highest band gap energy was obtained by 0.015 and 0.02 M K<sup>+</sup>doped ZnO nanoparticles. The band gap narrowing was necessary to absorb photons with a wide range of energies, so Li<sup>+</sup> doped ZnO nanoparticles was used to absorb photons in the portion of the solar irradiance with a high intensity than other dopants (Na<sup>+</sup> and K<sup>+</sup>).

**Keywords:** ZnO nanoparticles, Band gap energy, Alkali metals, Doping, UV-vis spectroscopy.

## 1. INTRODUCTION

Zinc oxide is an inorganic compound with the formula ZnO. It is a white powder that is insoluble in water, and it is widely used as an additive in numerous materials and products including rubbers, plastics, ceramics, glass, cement<sup>1</sup>, lubricants, paints, ointments, adhesives, sealants, pigments, foods (as a source of Zinc in nutrient), batteries, ferrites, **diaper rashes**, **calamine cream**, anti-dandruff shampoos, antiseptic ointments, etc.<sup>2</sup>. It occurs naturally as the mineral zincite, but most zinc oxide is produced synthetically<sup>3</sup>. It has become attractive as a semiconductor for DSSC since it can be easily fabricated with various nanostructures at low temperatures and has higher electron mobility than that of TiO<sub>2</sub>. However, it is less chemically stable than TiO<sub>2</sub> and may necessitate an additional layer for protection from the electrolyte<sup>4</sup>. The wide band gap energy of ZnO greatly limits the light responding range, which can only absorb ultraviolet light ( $\lambda < 380$  nm) and seriously limits the photo catalytic efficiencies. It has become an important issue to expand the visible light response of ZnO for practical applications<sup>5</sup>.

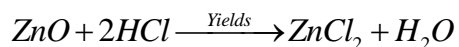
The band gap of ITO is about 3 eV that it absorbs the light which wavelength shorter than 400 nm seriously that the transmittance of ITO in UV region would be low<sup>6</sup>. The band gap of TiO<sub>2</sub> is about 3.2 eV which is treated as a wide band gap semiconductor can just be activated under ultraviolet irradiation ( $\lambda < 387$  nm), which occupies only about 5% of solar energy<sup>7</sup>. ZnO is regarded as an ideal alternative material for ITO because of its lower cost and easier etch ability<sup>8</sup>. The native doping of the semiconductor due to oxygen vacancies or Zinc interstitials is N-type<sup>9</sup>. In comparison with Si semiconductor, which is widely used in the display industry, metal oxide semiconductors show high electrical performance as well as unique properties, including good transparency, high electron mobility, wide band gap and strong room temperature luminescence. Those properties are used in emerging applications for transparent electrodes in liquid crystal displays; in energy saving or heat protecting windows and in electronics as thin film transistors and light-emitting diodes.

ZnO is biocompatible which makes it suitable for biomedical applications. Last but not least, it is a chemically stable and environmentally friendly material that have been used extensively for purpose of applications as microbial inhibition, photo catalysis, solar cells, removal of heavy metals, gas sensors, piezoelectric devices, anti-reflecting coatings, in lasers, detectors, flat panel displays, surface acoustic waves, etc<sup>10</sup>. Also used in phototherapy agents, owing to a wide band gap (3.37 eV), large exciton binding energy (60 meV) and semiconductor properties<sup>11</sup>.

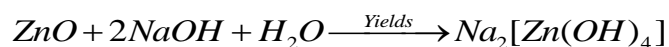
All Photovoltaic cells consist basically of a semiconductor material capable of absorbing a certain portion of the solar spectrum and adjacent layers (electrodes) required to extract the photo-generated carriers for conveyance to an external electrical load. Therefore, the optical and electronic properties of each material in the Photovoltaic cell should be tuned to prevent unnecessary loss of incident photons through reflection and parasitic absorption, as well as, to minimize loss of the photo-generated power via recombination at trap states and electrical resistance losses<sup>12</sup>.

Pure ZnO presents as a white powder, but in nature it occurs as the rare mineral zincite, which usually contains manganese and other impurities that confer yellow to red color<sup>13</sup>. Its crystalline form is thermochromic, changing from white to yellow when heated and in air reverting to white on cooling. This color change is caused by small loss of oxygen to the environment at high temperatures to form the non stoichiometric  $Zn_{1-x}O$ , where at 800<sup>0</sup>C, X=0.00007<sup>14</sup>.

It is an amphoteric oxide and nearly insoluble in water, but it is soluble in most acids, such as Hydrochloric acid.



It is also soluble in bases to give soluble zincates;



Band gap energy is an energy range in a solid where no electron states can exist. In graphs of the electronic band structure of solids, the band gap energy generally refers to the energy difference in electron volt between the top of the valance band and the bottom of the conduction band in insulators and semiconductors. The band gap is the major factor determining the electrical conductivity of a solid. Substance with large band gaps are generally insulators, those with smaller but non zero band gaps are semiconductors, either have very small band gaps or none are called conductors because the valance and conduction bands are over lap.

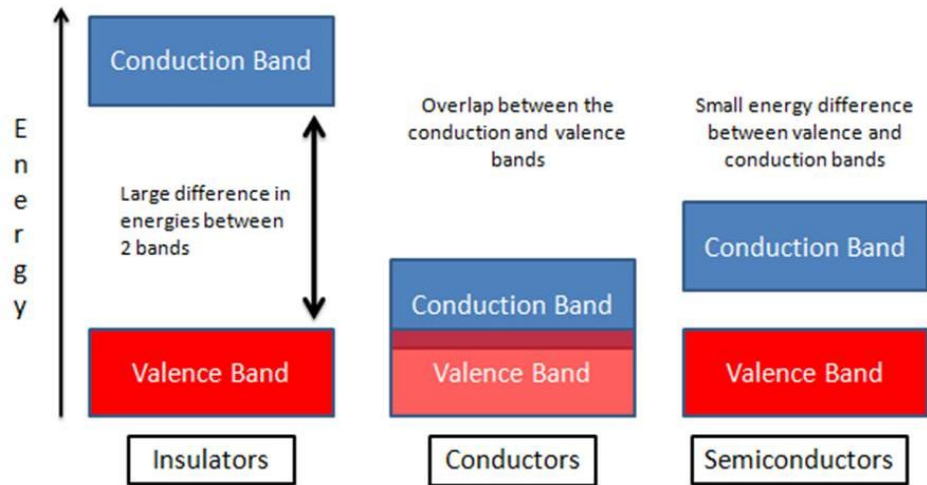


**Figure 1:** The differences between band gap of different Materials

Among the various dopants, alkali metals, such as  $\text{Li}^+$ ,  $\text{Na}^+$  and  $\text{K}^+$ , have received much attention due to their high field effect mobility, good electrical stability in TFTs and compatibility with a ZnO-based metal oxide semiconductor precursor solution<sup>15</sup>. It is well known that the changes in band gap energies could occur when impurities were added into a wide gap semiconductor and there is a higher degree of atomic homogeneity<sup>16</sup>. The group IA elements are used as doping materials to improve and tune the optical property and band gap energy of ZnO nanoparticles<sup>17</sup>. However, being smaller in atomic radii, group IA elements prefer to occupy the interstitial sites, rather than substitutional sites and therefore, act mainly as donors<sup>18</sup>.

## 2. REVIEW LITERATURE

### 2.1. Doping

Doping is the process of adding some impurity atoms in the semiconductors. These impurity atoms are known as dopants. After addition of these dopants some of the properties of the conductors can be changed according to our need.

- ❖ Cationic doping; The doping of a cation to metal oxide is known as cationic doping; e.g. Al, V, Cr, Mn, Fe, Ni<sup>19</sup>, Co<sup>20</sup> were used as cationic dopants to ZnO or TiO<sub>2</sub>.
- ❖ Anionic doping: The doping of an anion to metal oxide is known as anionic doping; e.g. N, C, and S<sup>21</sup> were used as anionic dopants to ZnO or TiO<sub>2</sub>.

In semiconductor production, doping intentionally introduces impurities into an extremely pure (also referred to as intrinsic) semiconductor for the purpose of modulating (adjusting) its electrical properties. The impurities are dependent upon the type of semiconductor. Lightly and moderately doped semiconductors are referred to as extrinsic<sup>16</sup>. A semiconductor doped to such high levels that it acts more like a conductor than a semiconductor is referred to as degenerate.

In an intrinsic semiconductor under thermal equilibrium, the concentration of electrons and holes is equivalent.

$$n = p = n_i$$

The conductivity of intrinsic semiconductors is strongly dependent on the band gap. The only charge carriers for conduction are the electrons that have enough thermal energy to be excited across the band gap and the electron holes that are left off when such an excitation occurs.

In non-intrinsic semiconductor in thermal equilibrium the relation becomes (for low doping):

$$n_o \cdot p_o = n_i^2$$

Where  $n_o$  is the concentration of conducting electrons,  $p_o$  is the electron hole concentration and  $n_i$  is the materials intrinsic carrier concentration.

In N-type material there are electrons energy levels near the top of the band gap so that they can be easily excited into the conduction band. In P-type material, extra holes in the band gap allow excitation of valence band electrons, leaving mobile holes in the valence band.

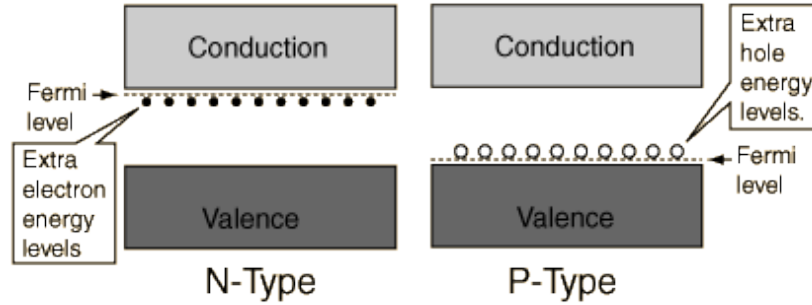
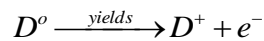


**Fig.2**The difference between N and P type dopants

### N-type doping

ZnO with a wurtzite structure naturally deviates from its stoichiometry, thus automatically forms an N-type semiconductor due to presence of intrinsic defects such as oxygen vacancies ( $V_o$ ) and Zn interstitials ( $Zn_i$ )<sup>22</sup>. Although it is experimentally known that unintentionally doped ZnO is N-type, whether the donor is Zn interstitials or oxygen vacancies. For N-type doping  $Zn^{2+}$  or  $O^{2-}$  should be replaced with atoms which contain one more electron in the outer shell. Thus, the group-IIIA elements Al, Ga and In can replace  $Zn^{2+}$  and group-VIIA elements  $Cl^-$  and  $I^-$  can be substitutional elements for  $O^{2-}$ <sup>23</sup>.



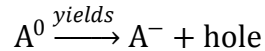
Where  $D^0$  and  $D^+$  are the neutral and ionized donors, respectively

### P-type Doping

It is very difficult to obtain P-type doping in wide-band-gap semiconductors such as GaN, ZnO and ZnSe. The difficulties to form shallow acceptor level arise mainly from (i) low solubility of the dopant in the host material, (ii) compensation of dopants by low energy native defects, like, Zn interstitials or oxygen vacancies or background impurities and (iii) deep impurity level.

To overcome those difficulties, one would expect that the P-type doping in ZnO may be possible by substituting either group IA elements like, Li, Na, and K for Zn sites or group-V elements as N, P, and As for oxygen sites<sup>24</sup>.

Group IA elements can act as deep acceptors with ionization energy around a few hundred meV<sup>25</sup>, which is much larger than  $k_B T$  at room temperature, According to the following equation;



Where  $A^0$  and  $A^-$  are the neutral and ionized acceptors. It has been shown that group-Ielements could be better  $p$ -type dopants than group-V elements in terms of shallowness of acceptor levels. Known  $P$ -type dopants include group-IA elements; group-V elements N, P and As; as well as copper and silver. However, many of these form deep acceptors and do not produce significant  $p$ -type conduction at room temperature.

### 2.1.1. Optical properties

Optical property of a material is defined as its interaction with electro-magnetic radiation in the visible. Materials are classified on the basis of their interaction with visible light into three categories.

Materials that are capable of transmitting light with relatively little absorption and reflection are called transparent materials. Translucent materials are those through which light is transmitted diffusely i.e. objects are not clearly distinguishable when viewed through. Those materials that are impervious to the transmission of visible light are termed as opaque materials. These materials absorb all the energy from the light photons.

Zinc oxide is transparent to visible light but strongly absorbs ultra violet light below 3655 Å<sup>0</sup>. The absorption is stronger than other white pigments. In the visible region wavelengths, regular zinc oxide appears white. Under ultra violet light zinc oxide is photoconductive. The combination of optical and semiconductor properties make doped zinc oxide a candidate for new generations of devices. Solar cells require a transparent conductive coating, indium tin oxide and doped zinc oxide are the best materials.

UV–visible absorption spectroscopy is a powerful technique to explore the optical properties of semiconducting nanoparticles. The absorbance is expected to depend on several factors such as band gap, oxygen efficiency, surface roughness and impurity centers<sup>26</sup>.

### 2.1.2. Effect of doping on band gap energy

The band gap for pure ZnO is found to be  $E_g \approx 3.35$  and for V doped ZnO samples of 1, 5 and 9 % V, was 3.24, 3.25 and 3.30 eV respectively. The band gap of all the V doped samples was lower than the pure ZnO sample. The reason for this decrease in band gap may be explained on the basis of alloying effect between ZnO and  $V_2O_5$ . The band gap of  $V_2O_5$  was 2.3 eV and ZnO was 3.37 eV. When  $V_2O_5$  was doped in ZnO, mixed oxide of  $ZnV_2O$  was formed and causes the decrease in the band gap energy. However, increase in doping concentration led to increase in band gap value which indicates that the Burstein–Moss effect is dominating for higher concentrations<sup>27</sup>.

The crystallite size decreases with the increase in Co concentration up to 5%  $C_o$  doping. Energy band gap varies from 1%, 3.46 eV to 5%, 3.57 eV with Co doping values are higher as compared to bulk ZnO (3.37 eV)<sup>28</sup>. The effect of oxygen vacancy on the energy gap of the ZnO samples prepared under different conditions, the optical properties of ZnO and ZnO samples were probed by UV-visible diffuse reflectance spectroscopy. The oxygen vacancies can effectively extend the visible light absorption of ZnO and the band gap narrowing was closely related to the oxygen vacancy concentration the high concentration of oxygen vacancy creates an impurity level near the valence band and induces the band gap narrowing<sup>5</sup>.

The optical absorption spectra of undoped and nickel doped zinc oxide ( $Zn_{1-x}Ni_xO$  where,  $x = 0.00, 0.05$ ) samples by UV-vis spectrophotometer in the range of 200 to 800 nm were performed. It was observed that the excitonic absorption peak of as prepared undoped and nickel doped samples appears around 260 nm which was fairly blue shifted from the absorption edge (i.e. much below the band gap wavelength of 365 nm,  $E_g = 3.4$  eV) of bulk ZnO<sup>29</sup>. The band gap decreases from 3.05 eV to 2.95 eV with Nickel (5%) doping at temperature 400°C. The absorption edge values of as prepared undoped and nickel doped samples were found to increase with increase in temperature from 300 to 800°C but the band gap values of as prepared undoped and nickel doped samples were found to decrease with increase in temperature from 300 to 800°C<sup>29</sup>.



The particle size can be adjusted by controlling the reaction temperature. The average size of nanoparticles increases as the heating temperature is increased and decreases as the doping percentage of nickel metal is increased. The strongest absorption peak appears at around 260 nm, which is blue shifted from the absorption edge of bulk ZnO (365 nm). The band gap value of prepared undoped and nickel doped ZnO nanoparticles decreases as annealing temperature increased from 300 to 800°C. Optical absorption measurements indicate red shift in the absorption band edge upon Ni doping<sup>29</sup>.

For Ni doped ZnO films the energy gap decreases from 2.95 to 2.72 eV as the [Ni]/[Zn] ratio increases from 0 to 0.02 and then increases to reach 3.22 eV for [Ni]/[Zn] = 0.04. The decrease of the band gap is attributed to the formation of defect energy level of Ni. It is established that Ni acts as donor impurity, which produces a shallow donor level below the conduction band, reducing the band gap of ZnO. On the other hand, the increase of the band gap energy when the [Ni]/[Zn] ratio varies from 0.02 to 0.04 is resulted to the reduction of the tail in the valence and conduction bands<sup>30</sup>.

The value of the band gap energy of undoped nanocrystalline ZnO nanoparticles was 3.26 eV and increased by incorporation of Sb doping as it was 3.309 eV for doping 1% Sb, 3.318 eV for 3% Sb and 3.329 eV for 5% Sb. This enhancement in band gap is due Sb incorporation and the high carrier concentration that moved the optical absorption edge towards lower energy and broadened the energy gap<sup>31</sup>.

Metal oxide semiconductors show high electrical performance as well as unique properties such as transparence induced by the wide bandgap<sup>32</sup>. In the ZnO-based metal oxide semiconductors TFTs, UV-visible spectroscopy analysis can be simply used as analysis tool because of their unique optical property like transparence<sup>33</sup>.

## 2.2. Statement of the problems

Pure ZnO was N-type semiconductor, but its optical property and band gap energy seem to be not very stable and have high resistivity or low conductivity, at room temperature, due to its wide band gap energy and high exciton-binding energy but when it was doped with alkali metals its optical and band gap energy can be very stable and used as starting material in solar cell, because alkali Metals doping was an energetically endothermic process ascribed to the smaller charge density on its ions in comparison with alkaline earth metal ions or N-type ZnO could be realized by doping with alkali metals to adjust its optical property (conductivity) and band gap energy.

This research will give answers for the following questions;

- Which of the alkali metals ( $\text{Li}^+$ ,  $\text{Na}^+$  and  $\text{K}^+$ ) used to serve as dopant for ZnO provides a narrow band gap?
- What should be lowest band gap energy of alkali metals doped ZnO?

## 2.3. Objectives of the study

### 2.3.1. General objective

- ❖ The objective of this work is to band gap narrowing of ZnO using  $\text{Li}^+$ ,  $\text{Na}^+$  and  $\text{K}^+$  metal ions by varying concentration and to discuss its optical property

### 2.3.2. Specific objectives

- ❖ To synthesis ZnO nanoparticles and determine its band gap energy
- ❖ To determine appropriate concentration of  $\text{Li}^+$ ,  $\text{Na}^+$  and  $\text{K}^+$  as dopant that affect more on ZnO nanoparticles band gap energy
- ❖ To study optical property of doped ZnO

#### **2.4. Significance of the study**

This study was expected to contribute knowledge to know which appropriate concentration of  $\text{Li}^+$ ,  $\text{Na}^+$  and  $\text{K}^+$  doped ZnO nanoparticles more narrow the band gap of undoped ZnO nanoparticles. In its pure form, zinc oxide was an N-type semiconductor, i.e., conductivity by electrons but, by doping with other elements to replace either the zinc or the oxygen; the conductivity can be varied over a very wide range. Doping of a certain amount in to ZnO matrix has become an important route to optimize its optical band gap energy. The band gap narrowing was necessary to absorb photons with a wide range of energies, most especially, in that portion of the solar irradiance with high intensity.

### 3. MATERIALS AND METHODS

#### 3.1. Chemicals

Zinc Acetate dihydrate ( $\text{Zn}(\text{CH}_3\text{COOH})_2 \cdot 2\text{H}_2\text{O}$ ) (Finken, 98%), Sodium hydroxide (NaOH) (Finken, 97%), Lithium Nitrate ( $\text{KNO}_3$ ) (Nice, 97%), Sodium Nitrate ( $\text{NaNO}_3$ ) (Nice, 97%), Potassium Nitrate ( $\text{KNO}_3$ ) (Nice, 97%), Ethanol (Hylux, 98%), Deionized water and Distilled water.

#### 3.1.1 Instrument and materials

Analytical balance, Oven, Volumetric flask, Measuring cylinder, Ultrasonic wave irradiation, Quartz cuvet, Hot plate and JENWAY 6705 UV-visible spectrophotometer

#### 3.2. Procedures

##### 3.2.1. Preparation of ZnO nanoparticles

50 mL of aqueous solution of 0.2 M Zinc acetate dihydrate ( $\text{Zn}(\text{CH}_3\text{COOH})_2 \cdot 2\text{H}_2\text{O}$ ) was added to 10 mL of aqueous solution of 0.2 M Sodium hydroxide (NaOH) and subjected to ultrasonic wave irradiation for 2 hr. The obtained white precipitate was filtered and washed with Deionized water and ethanol and dried in an oven at  $60^\circ\text{C}$  for 2 hr. Then sample was calcined (heated) at  $400^\circ\text{C}$  for 2 hr to evaporate the solvent and remove organic residuals. The solution was carried out using JENWAY 6705 UV-visible spectrophotometer.

##### 3.2.2. Preparation of Sodium, lithium and potassium ions doped ZnO nanoparticles

0.02 M of  $\text{LiNO}_3$ ,  $\text{NaNO}_3$  and  $\text{KNO}_3$  was each prepared in 50 mL of deionized water and the serial dilution ( $M_1V_1 = M_2V_2$ ) of 0.005 M, 0.01 M and 0.015 M was prepared in 10 mL of deionized water for each dopants. 10 mL of each concentration was doped to ZnO nanoparticles, then each solution of doped ZnO nanoparticles was calcined at  $400^\circ\text{C}$  for 2 hr and then each powder was prepared in 100 mL of deionized water. Absorbance measurement was carried out to characterize doped ZnO nanoparticles by UV-Vis spectroscopy to determine their band gap energy from Tauc's relationship by extrapolating straight line along the x-axis.

## 4. RESULTS AND DISCUSSION

### 4.1. Absorption spectrum

A spectrophotometer was used to measure the amount of light absorbed by a substance. An absorption spectrum was the plot of the absorbance versus the wavelength of the incident light.

#### 4.1.1. Characterization of ZnO nanoparticles

UV-visible spectrophotometer is widely used techniques to examine the optical properties of nanosized particles. In this work, deionized water was used as a blank for adjusting the instrument. Then the absorbance of the ZnO nanoparticles solution was measured using a quartz tube. The UV-vis absorption spectra of the samples were recorded in the wavelength range of 260 to 500 nm using, and Figure 3, illustrates the UV-vis spectrum of ZnO nanoparticles.

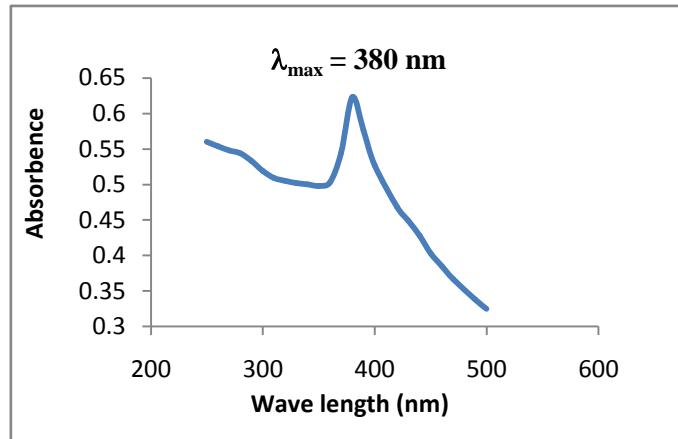


**Figure 3:** UV-vis absorption spectrum of ZnO nanoparticles

As can be seen, from the figure, ZnO nanoparticles exhibited maximum absorption of 380 nm, indicating red shift when compared with the bulk powder of ZnO, (absorption maxima, 365 nm). This can be assigned to the intrinsic band gap absorption of ZnO due to the electron transitions from the valence band to the conduction band<sup>34</sup>.

## Tauc's law plot of ZnO nanoparticles

This plot was used to determine the band gap energy by extrapolating straight line to the x-axis. Fig. 4, shows Tauc's law plot of ZnO nanoparticles, Which was constructed as  $(\alpha hv)^2$  as a function of photon energy ( $hv$ ) of the nanoparticles.

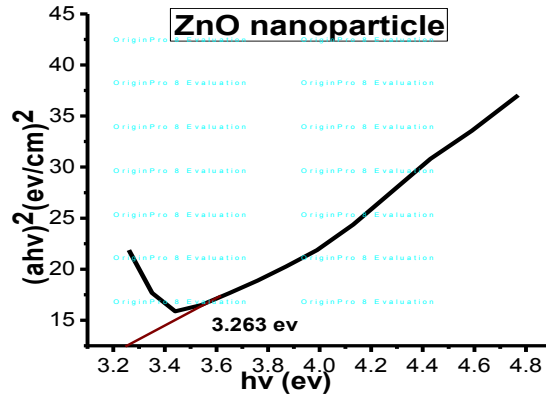


**Figure 4:** Plots of  $(\alpha hv)^2$  versus photon energy ( $hv$ ) of ZnO nanoparticles

The optical band gap energy of the nanoparticles was determined by applying the Tauc's relationship<sup>35</sup>.

$$(\alpha hv) = c(hv - E_g)^{1/2} \quad (1)$$

Where;  $\alpha$  is the optical absorption coefficient ( $\alpha = 2.303 \frac{A}{t}$  here,  $A$  is the absorbance and  $t$  is the thickness of the cuvette),  $E_g$  is the band gap energy,  $hv$  is the energy of the radiation (photon energy),  $c$  is a constant that is independent of the photon energy. As can be seen from the Fig. 4 the band gap energy of the prepared ZnO nanoparticles was  $\approx 3.263$  eV, which is narrower than that of the bulk (3.37 eV). Nanoparticles show lattice contraction due to high attractive electrostatic interaction between  $Zn^{2+}$  and  $O^{2-}$  ions.

The size of the particle was obtained from the absorbance spectra by calculating using formula, which was derived from effective mass model. As compared to bulk ZnO powder, the absorption edge of prepared ZnO nanoparticles was systematically shifted to higher wavelength (red shifted) or lower band gap energy with increasing size of the nanoparticles. This pronounced and systematic shift in the absorption edge was due to the quantum size effect<sup>36</sup>.

The following equation was derived using the effective mass model to determine the particle size (radius) as a function of peak absorbance wavelength ( $\lambda_p$ ) for the mono dispersed ZnO nanoparticles;

$$r_{(nm)} = \frac{-0.3049 + \sqrt{-26.23012 + \frac{10240.72}{\lambda_p}}}{-6.3829 + \frac{2483.2}{\lambda_p}}$$

$$E = E_g^{\text{bulk}} + \frac{h^2\pi^2}{2\mu r^2} - 1.8 \frac{e^2}{\epsilon r} - 0.248 E_{RY}^*, \text{ Where}$$

$$\frac{1}{\mu} = \frac{1}{m^*_e} + \frac{1}{m^*_h}$$

$$E_{RY}^* \text{ in } m^{-1} = \frac{m_e e^4}{8\epsilon_0^2 h^3 C}$$

$$E_{RY}^* \text{ in eV} = E_{RY}^* hc$$

where,  $E_{RY}^*$ , is the effective Rydberg energy,  $E_g^{\text{bulk}}$  is the bulk band gap energy ( $\approx 3.37$  eV),  $\mu$  is the reduced mass,  $r$  is sphere radius (particle size),  $h$  is Plank's constant ( $6.626 \times 10^{-34}$  m<sup>2</sup>kg/s),  $m^*_e$  is the electron effective mass (0.26),  $m^*_h$  is the hole effective mass (0.59), It has been referred that the band gap enlargement is expected for ZnO nanoparticles size of much less than 4 nm<sup>37</sup>. In this work, the prepared ZnO nanoparticles have a particle size of 3.6 nm, which was almost equal to 4 nm, indicating no expectation for band gap enlargement.  $e$  is the charge on the electron ( $1.602 \times 10^{-19}$  C),  $\epsilon_0$  is the permittivity of free space ( $8.85 \times 10^{-12}$  (F/m) and  $\epsilon$  is the relative permittivity (8.5). In effective mass formula, the first term on the right hand side represents the band gap of bulk materials, The second additive term of the equation represents the additional energy due to quantum confinement having  $1/r^2$  dependence on band gap energy and the third subtractive term stands for the columbic interaction energy of exciton having  $1/r$  dependence on band gap energy, often neglected due to high dielectric (relative permittivity) constant of the material<sup>38</sup>.

## **4.2. Optical properties of different concentration of Li<sup>+</sup>, Na<sup>+</sup> and K<sup>+</sup> doped ZnO**

The magnitude of bandgap shift due to moderate or heavy doping level was determined by two competing mechanisms; bandgap narrowing (BGN) which was a consequence of many body effects on the conduction and valence bands and the bandgap widening (BGW) which was referred to the well known Burstein–Moss effect.

### **4.2.1. Characterization of Li<sup>+</sup>, Na<sup>+</sup> and K<sup>+</sup> doped ZnO nanoparticles**

The maximum absorption peak of each concentration was determined from their corresponding spectra. The UV–Visible absorption spectra of different concentration Li<sup>+</sup>, Na<sup>+</sup>, K<sup>+</sup> doped and undoped ZnO nanoparticles was shown in Figure 5, table 1. In all cases, the obtained results demonstrated that the absorption maxima's of nanoparticles were changed with the change of the type of the dopants and as well as their concentrations. The absorption maxima presents the wavelength at which take place between valence and conduction bands<sup>39</sup>. The dopant that have larger wavelength was red shifted, with decreasing the band gap energy of undoped ZnO nanoparticles. From all those dopants 0.015 M Li<sup>+</sup> doped ZnO nanoparticles have highest wavelength and narrow band gap. 0.02 M K<sup>+</sup> doped ZnO nanoparticles have lowest wavelength than others that means it was blue shifted due to its larger ionic size and low electronegativity.



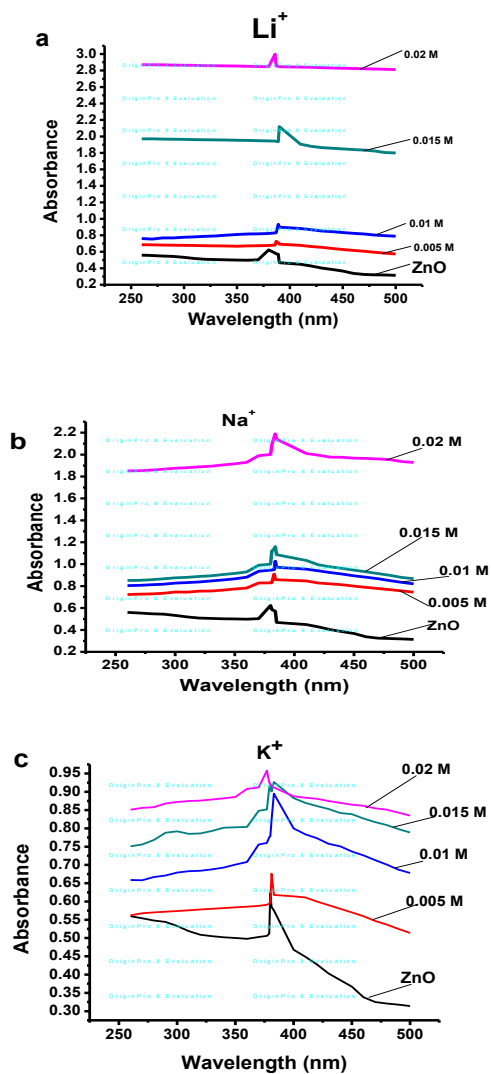


**Fig 5:** The UV–Visible absorption spectra of a)  $\text{Li}^+$ , b)  $\text{Na}^+$  and c)  $\text{K}^+$  doped and undoped ZnO nanoparticles

**Table 1** Maximum absorption peaks of different concentration doped ZnO nanoparticles

Dopants	$\lambda_{\text{max}}$ (nm)				Undoped ZnO $\lambda_{\text{max}} =$ <b>380 nm</b>
	0.005 M	0.01 M	0.015 M	0.02	
$\text{Li}^+$	387	389	390	386	
$\text{Na}^+$	383	385	384	381	
$\text{K}^+$	381	383	379	377	

### 4.3. Effect of doping on band gap energy of ZnO nanoparticles

Plots of  $(\alpha h\nu)^2$  vs  $h\nu$  for undoped ZnO nanoparticles and 0.005, 0.01, 0.015 and 0.02 M of  $\text{Li}^+$ ,  $\text{Na}^+$  and  $\text{K}^+$  doped ZnO nanoparticles was shown in figure, 6, Table 2. The obtained results demonstrated that the band gap energy of  $\text{Li}^+$  doped ZnO nanoparticles decrease with increasing concentration of the dopant  $\text{Li}^+$ . This might be attributed to the increase of oxygen vacancies, resulting from introduction of  $\text{Li}^+$  at  $\text{Zn}^{2+}$  sites<sup>40</sup>.

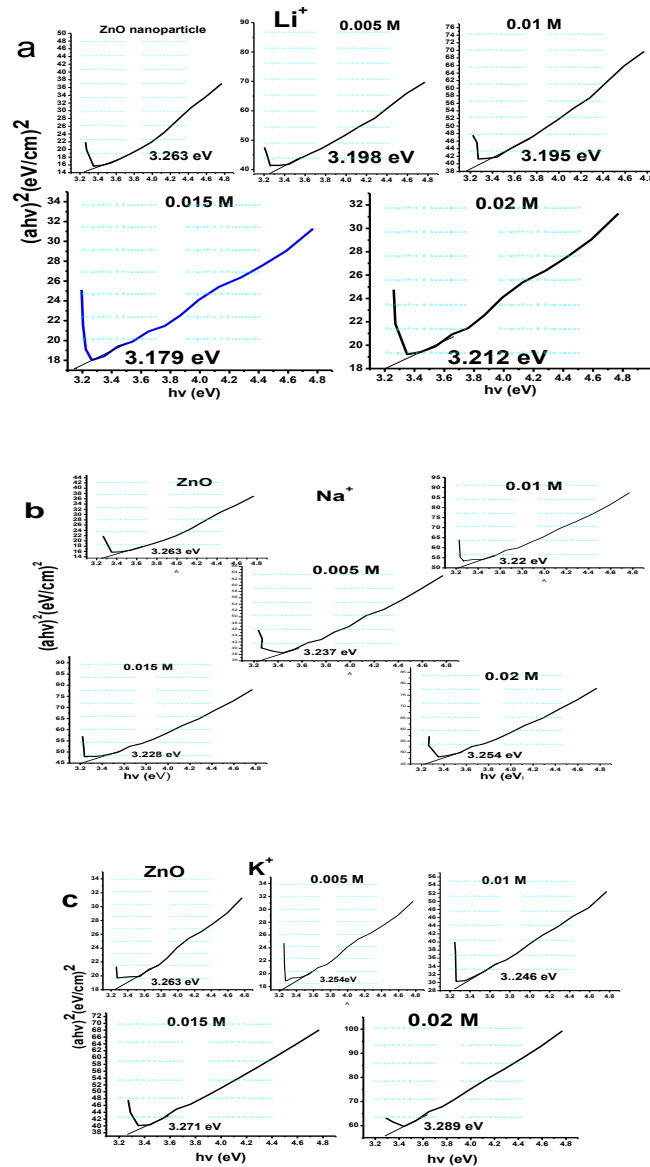


**Fig. 6,** Plots of  $(\alpha h\nu)^2$  vs  $h\nu$  for undoped ZnO nanoparticles and different concentrations of a)  $\text{Li}^+$ , b)  $\text{Na}^+$  and c)  $\text{K}^+$  doped ZnO nanoparticles.

**Table 2:** The band gap energy of undoped and different conc. of Li<sup>+</sup>, Na<sup>+</sup> and K<sup>+</sup> doped ZnO nanoparticles

Metal ion	Ionic Size (nm)	Band gap (eV)			
		0.005M	0.01M	0.015M	0.02
Li <sup>+</sup>	0.068	3.198	3.195	3.179	3.212
Na <sup>+</sup>	0.097	3.237	3.22	3.228	3.254
K <sup>+</sup>	0.133	3.254	3.237	3.271	3.289
Zn <sup>2+</sup>	0.074	-	-	-	-

For all different concentrations the band gap energy indicating minimum band gap energy for the smaller ion, Li<sup>+</sup> and the highest for the largest ion, K<sup>+</sup>, among the studied dopant, alkali metals. So Na<sup>+</sup> and K<sup>+</sup> due to doped ZnO nanoparticles its smallest ionic radii and highest electronegativity of Na and K<sup>41</sup>, it attracts bonding electrons strongly than others, Na<sup>+</sup> and K<sup>+</sup>, its lower ionic radii of Li<sup>+</sup> than Zn<sup>2+</sup>. Moreover, its higher electronegativity then demonstrated the highest change in the conductivity of Li<sup>+</sup> doped ZnO nanoparticles.

From all dopants 0.015 and 0.02 M K<sup>+</sup> doped ZnO nanoparticles the band gap energy of undoped ZnO nanoparticles increases from 3.263 to 3.271 and 3.289 eV respectively. The larger size as well as concentration of the dopant increases the band gap energy, due to the Fermi level to push to conduction band above edge and such doping induced band-filling called as Burstein Moss shift. So the contribution of K<sup>+</sup> ions on interstitial sites of Zn<sup>2+</sup> ion determines the widening of the band gap caused by an increase in carrier concentration (donor electrons)<sup>41</sup>.

The difference in band gap of undoped and doped ZnO nanoparticles was observed due to the incorporation of dopants in ZnO lattice. As the size and concentration of dopant increases, Oxygen vacancy decreases, because the opportunity of freely moving electrons from valance band to conduction band decreases. That means the introduction of larger size dopant enhances the crystallinity of ZnO nanoparticles, and hence band gap energy increases. Undoped ZnO nanoparticles have conductivity by electrons, but when it is doped with different concentration of Li<sup>+</sup>, Na<sup>+</sup> and K<sup>+</sup> its conductivity is varied.

Red-shift of fundamental absorption edge was observed when the band gap energy was narrowed in comparison to undoped ZnO nanoparticles. The band gap narrowing was observed due to merging of an impurity band into the conduction band, thereby shrinking the band gap. Formation of such impurity band giving rise to new donor electronic states just below the conduction band was possible and this arises due to hybridization between states of the ZnO matrix and that of the dopants<sup>42</sup>.

#### **4.4. Comparison of the obtained results with reported values**

The obtained results for  $\text{Li}^+$  and  $\text{K}^+$  were compared with other reported values for ZnO thin films doped with  $\text{Li}^+$  and  $\text{K}^+$  was shown, in Table 3. The band gap energy of the undoped thin films of ZnO were lower than the doped products with either  $\text{Li}^+$  and  $\text{K}^+$  doped ZnO thin films<sup>43,44</sup>. Moreover, with the an increase in the concentrations of dopants,  $\text{Li}^+$  or  $\text{K}^+$ , though, the band gap energy has slightly shown a decrement, it cannot lower than the band gap energy of undoped ZnO thin films. However, in this study, it was observed that the band gap energy of ZnO nanoparticles has narrowed when the nanoparticles was doped with either  $\text{Li}^+$  or  $\text{K}^+$ . Besides, the band gap energy of the studied nanoparticles has also shown smaller band gap than the undoped ZnO nanoparticles. In general, the findings of the present study revealed that use of alkali metals as a dopant for ZnO nanoparticles exhibited reduction of the band gap energy.

**Table 3:** Comparative study of Li<sup>+</sup> and K<sup>+</sup> doped ZnO thin films from literature and doped ZnO nanoparticles for this work

mol%	band gap energy (eV)	dopant	type	Ref.
undoped ZnO	3.264	Lithium	(ZnO: Li <sup>+</sup> ) thin film	
1	3.287			
10	3.298			
15	3.286			
%				
undoped ZnO	3.8	Potassium	(ZnO: K <sup>+</sup> ) thin film	
1	3.94			
2	3.89			
4	3.86			
<b>Concentration (M)</b>				
undoped ZnO	3.263	Lithium	(ZnO: Li <sup>+</sup> ) nanoparticles	This work
0.005	3.198			
0.01	3.195			
0.015	3.179			
0.005	3.254	Potassium	(ZnO: K <sup>+</sup> ) nanoparticles	
0.01	3.237			
0.015	3.271			

## 5. CONCLUSSION

ZnO nanoparticles were prepared from Zinc acetate and Sodium hydroxide by precipitation method and the solution was characterized by UV-visible spectrophotometer. The nanoparticles exhibited maximum absorbance of 380 nm and its optical band gap energy was  $\approx 3.263\text{eV}$  that was narrower than the band gap of bulk ZnO powder (3.37 eV). The resulted difference in band gap energy shows the prepared ZnO was nanoparticles. As particle size decrease the absorption edge shifts to lower wavelength or higher band gap energy. As the dopants ionic size increases, the band gap energy of ZnO nanoparticles also increases, because of the lowering of oxygen vacancy. From the studied dopants 0.015 M  $\text{Li}^+$  doped ZnO nanoparticles were influenced (more narrowed) the band gap energy of undoped ZnO nanoparticles than  $\text{Na}^+$  and  $\text{K}^+$  doped ZnO nanoparticles. The band gap energy of undoped ZnO nanoparticles was affected by ionic size, electronegativity and concentration of dopants.

## References

1. Sanchez-Pescador, R.; Brown, J. T.; Roberts, M.; Urdea, M. S., The nucleotide sequence of the tetracycline resistance determinant tetM from *Urea plasma urea lyticum*. *Nucl. Acid. Res.* **1988**, *16*, 1216.
2. Hernandezbattez, A. G. R. V. J.; Fernandez, J.; Diazfernandez, J.; Machado, A.; Chou, R.; Riba, J., CuO, ZrO<sub>2</sub> and ZnO nanoparticles as antiwear additive in oil lubricants *Appl. Mater.* **2008**, *265*, 422.
3. Liedekerke, M. D., 2.3. Zinc oxide (zinc white): Pigments, Inorganic. *Ullmann's Encycl. Indus. Chem.* **2006**, *4*, 15-17.
4. Yih, L. C.; Tung, Y. Y., Hierarchically assembled ZnO nanoparticles. *Roy. Soc. Chem.* **2013**, *5*, 1777-1780.
5. Wang, J.; Wang, Z.; Huang, B.; Ma, Y.; Liu, Y.; Qin, X.; Zhang, X.; Dai, Y., Oxygen vacancy induced band-gap narrowing and enhanced visible light photocatalytic activity of ZnO. *ACS Appl. Mater. Interfaces* **2012**, *4*, 4024-4030.
6. Kim, Y. S.; Lee, L. J., Highly reflective and low-resistant Ni/Au/ITO/Ag ohmic contact on p-type GaN. *Electrochem. Solid-state. Lett.* **2004**, *7*, 102-104.
7. Yan, H.; Wang, X.; Yaon, M.; Yao, X., Band structure design of semiconductors for enhanced photocatalytic activity. *Mater. Int.* **2013**, *23*, 402-407.
8. Pan, Z. W.; Dai, Z. R.; Wang, Z. L., Nanobelts of semiconducting oxides. *Sci.* **2001**, *291*, 1947.
9. Özgür, Ü. A. Y. I.; Liu, C.; Teke, A.; Reshchikov, M. A.; Doğan, S.; Avrutin, V.; Cho, S. J.; Morkoc, H. A., Comprehensive review of ZnO materials and devices. *J. Appl. Phys.* **2005**, *98*, 041301.
10. Pei, G.; Xia, C.; Wang, L.; Xing, L.; Jiao, X.; Xu, J., Synthesis and characterizations of Al-doped ZnO, *Scrip. Mater.* **2007**, *56*, 967-970
11. Imai, Y.; Watanabe, A., Comparison of electronic structures of doped ZnO by various impurity elements calculated by a first-principle pseudopotential method, *Mater. Sci.* **2004**, *15*, 743-749.
12. Sonya, C., Applications of oxide coatings in photovoltaic devices. *Coatings*, **2014**, *4*, 162-202.

13. Klingshirn, C., ZnO: Material, Physics and Applications. *Chem. Phys. Chem*, **2007**, *8*, 782- 803.
14. Wiberg, E.; Holleman, A. F., Disinfection performances of stored acidic and neutral electrolyzed waters generated from brine. *Inorg. Chem.* **2001**, *1*, 442-448.
15. Park, S. Y.; Kim, B. J.; Kim, K.; Kang, M. S.; Lim, K. H.; Lee, T. I.; Young, J. M.; Baik, H. K.; Cho, J. H.; Kim, Y. S., Low temperature, solution processed and alkali metal doped ZnO for high performance thin film transistors. *Adv. Mater.* *24* , 834-838.
16. Moezzi, A.; Mcdonagh. A. M.; Cortie.; M. B., Review: Zinc oxide particles: synthesis, properties and applications. *J. Chem. Eng.* **2012**, *1-22*, 185-186.
17. Shanmuganathan, G.; Banu, I. S., Studies on the optical constants of K and Fe codoped ZnO thin films prepared by chemical bath deposition. *Innov. Res. Sci. Technol.***2000**, *4*, 5.
18. Chawla, S.; Jayanthi, K.; Kotnala, R. K., Room-temperature ferromagnetism in Li<sup>+</sup> doped P-type luminescent ZnO nanorods. *Phys. Rev. B* **2009**, *79*, 125-204.
19. Colis, S.; Bieber, H.; Begin-Colin, S.; Schmerber, G.; Leuvrey, C.; Dinia, A., Magnetic properties of Co-doped ZnO diluted magnetic semiconductors prepared by low temperature mechano synthesis. *Chem. Phys. Lett.* **2006**, *42*, 529–533.
20. Xu, C., Cao, L.; Su, G.; Liu, W.; Qu, X.; Yu, Y., Preparation, characterization and photocatalytic activity of Co-doped ZnO powders. *J. Alloys Comp.* **2010**, *497*, 373-376.
21. Wong, M. S.; Chou, P.H.; Yang, T. S., Reactively sputtered N-doped titanium oxide films as visible-light photo catalyst. *Thin Solid Films*, **2006**, *494*, 1-2.
22. Park, C. K.; Ma. Y. D.; Kim, H. K., Physical properties of Al doped zinc oxide films prepared by RF magnetron sputtering. *Thin solid Films*, **1997**, *305*, 201-209.
23. Kato, H.; Sano, M.; Miyamoto, K.; Yao, T., Growth and characterization of Ga-doped ZnO layers on a-plane sapphire substrates grown by molecular beam epitaxy. *J. Crys. Growth* **2002**, *538*, 237-239.
24. Wei, S. H.; Zhang, S. B., Chemical trends of defect formation and doping limit in II-VI semiconductors. *Phys. Rev. B.* **2002**, *66*, 073202.
25. Zwingel, D.; Gartner, D. F., Paramagnetic and optical properties of Na doped ZnO single crystals. *Solid State Commun.* **1974**, *14*, 45.



26. Ahmed, A. S.; Singla, M. L.; Tabassum, S ; Naqvi, A. H.; Azam, A.; Lumin., Band gap narrowing and fluorescence properties of nickel doped SnO<sub>2</sub> nanoparticles. *J. Luminescence*, **2011** *131*, 1-6.
27. Joshi, R.; Kumar, P.; Gaur, A.; Asokan, K., Structural, optical and ferroelectric properties of V doped ZnO. *Appl. Nanosci.* **2014**, *4*, 531-536.
28. Ansari, S. A.; Nisar, A. A.; Fatma, B.; Khan, W.; Naqvi, A. H., Investigation on structural, optical and dielectric properties of Co doped ZnO nano particles synthesized by gel combustion route. . *Mater. Sci. Eng. B* **2012**, *177*, 428-435.
29. Elilarassi, R.; Chandrasekaran, G., Synthesis and optical properties Of Ni doped zinc oxide nanoparticles. *Optoelectronics Letters*, **2010**, *6*, 6-10.
30. Bouaoud, A.; Ramili, A.; Quachtari, F.; Louardi, A.; Chtouki, T.; Elidrissi, B.; Erguig, H., Transparent conducting properties of Ni doped zinc oxide thin films prepared by a facile spray pyrolysis technique using perfume atomizer. *Mater.Chem. Phy.* **2013**, *137*, 843-847.
31. Rana, S. B.; Singh, A.; Singh, S., Characterization and optical studies of pure and Sb doped ZnO nanoparticle. *Int. J. Nanoelectronics. Mater.* **2013**, *6*, 45-57.
32. Vacha, M.; Habuchi, S., Conformation and physics of of polymer chains: asingle molecule perspective. *NPG Asia Mater.* **2010**, *2*, 134-142.
33. Lim, K. H.; Kim, S.; Park, S. Y.; Kim, H.; Kim, Y. S., UV-visible spectroscopic analysis of electrical properties in alkali metal-doped amorphous zinc tin oxide thin-film transistors. *Adv. Mater.* **2013**, *25*, 2-3000.
34. Yu, J.; Yu, X., hydrothermal synthesis and photocatalytic activities of ZnO hollow spheres. *Environ. Sci. Technol.* **2008**, *42*, 4902-4907.
35. Tauc, J., Amorphous and liquid semiconductors. *Plenum Press, New York*, **1974**, *1*, 171.
36. Pesika, N.S. S.; Searson, K. J., Determination of the particle size distribution of quantum nanocrystals from absorbance spectra. *Adv. Matter* **2003**, *15*, 1289-1291.
37. Satyanarayana, T. S. R. K.; Nagarjuna, G., Synthesis, characterization, and spectroscopic properties of ZnO nanoparticles. *Int. Schol. Res. Network*, **2012**, *1*,6.
38. Changiz, V. A. E., Quantum size effects on effective mass and band gap of semiconductor quantum dots. *Res. J. Recent Sci.* **2013**, *2*, 21-24.

39. Sunil, C. M. K.; Sandeep, C.; Katyal, S. C.; Awana, V. P. S., Structural, vibrational, optical and magnetic properties of sol-gel derived Nd doped ZnO nanoparticles. *J. Mater. Sci. Mater. Electron.* **2013**, *24*, 5102-5110.
40. Maa, Q. Z. Y.; Zhang, A.; Lu, M.; Zhou, G.; Li, C. , Synthesis and optical properties of novel red phosphors YNbTiO<sub>6</sub>:Eu<sup>3+</sup> with highly enhanced brightness by Li<sup>+</sup> doping. *Solid State Sci.* **2009**, *11*, 1124-1130.
41. Li, H. H. Y.; Li, Z.; Yao, Y.; Zhang, S., Preparation and infrared emissivities of alkali metal doped ZnO powders. *J. Cent. South Univ.* **2014**, *21*, 3449-3455.
42. Mondal, S. B. S. R.; Mitra, P., Effect of Al doping on microstructure and optical band gap of ZnO thin film synthesized by successive ion layer adsorption and reaction. *J. Phys.* **2013**, *80*, 315-326.
43. Park, S.Y.; Kim, K.; Lim, K.H.; Kim, B. J.; Lee, J. H. C.; Kim, S.Y., The structural, optical and electrical characterization of high performance, low temperature and solution processed alkali metal doped. *J. Mater. Chem. C*, **2013**, *1*, 1383.
44. Shamuganathan, G.; Shameem, I. B.; Krishnan, S.; Ranganathan, B., Influence of K doping on the optical properties of ZnO thin films grown by chemical bath deposition method. *J. Alloys Compds.* **2013**, *562*, 190.